The crystal structure of the globular domain of sheep prion protein

doi:10.1016/j.jmb.2003.12.059 J. Mol. Biol. (2004) 336, 1175–1183

JMB

Available online at www.sciencedirect.com

SCIENCE DIRECT®

ELSEVIER

The Crystal Structure of the Globular Domain of Sheep Prion Protein

L. F. Haire[1]†, S. M. Whyte[1]†, N. Vasisht[1], A. C. Gill[2], C. Verma[3,4] E. J. Dodson[3], G. G. Dodson[1,3] and P. M. Bayley[1]*

[1]*Structural Biology Group Division of Protein Structure National Institute for Medical Research, The Ridgeway, Mill Hill, London NW7 1AA, UK*

[2]*TSE Division, Institute for Animal Health, Compton Newbury RG20 7NN, UK*

[3]*York Structural Biology Laboratory, University of York York YO10 5YW, UK*

[4]*Bioinformatics Institute, 30 Biopolis Way, #07-01 Matrix Singapore 138671*

**Corresponding author*

The prion protein PrP is a naturally occurring polypeptide that becomes transformed from a normal conformation to that of an aggregated form, characteristic of pathological states in fatal transmissible spongiform conditions such as Creutzfeld–Jacob Disease and Bovine Spongiform Encephalopathy. We report the crystal structure, at 2 Å resolution, of residues 123–230 of the C-terminal globular domain of the ARQ allele of sheep prion protein (PrP). The asymmetric unit contains a single molecule whose secondary structure and overall organisation correspond to those structures of PrPs from various mammalian species determined by NMR. The globular domain shows a close association of helix-1, the C-terminal portion of helix-2 and the N-terminal portion of helix-3, bounded by the intramolecular disulphide bond, 179–214. The loop 164–177, between β2 and helix-2 is relatively well structured compared to the human PrP NMR structure. Analysis of the sheep PrP structure identifies two possible loci for the initiation of β-sheet mediated polymerisation. One of these comprises the β-strand, residues 129–131 that forms an intra-molecular β-sheet with residues 161–163. This strand is involved in lattice contacts about a crystal dyad to generate a four-stranded intermolecular β-sheet between neighbouring molecules. The second locus involves the region 188–204, which modelling suggests is able to undergo a partial $\alpha \rightarrow \beta$ switch within the monomer. These loci provide sites within the PrP^{c} monomer that could readily give rise to early intermediate species on the pathway to the formation of aggregated PrP^{Sc} containing additional intermolecular β-structure.

Keywords: transmissible spongiform encephalopathy; Creutzfeld–Jacob Disease; scrapie; X-ray crystallography; protein structure

The prion protein PrP occurs in a wide range of eukaryotic cells but its normal physiological function is unknown. However, mutant PrPs are associated with the development of transmissible spongiform encephalopathies (TSE). Notable examples of TSE include the bovine disease (BSE) and, in humans, new variant CJD. While an infectious agent has not been conclusively identified, the evidence suggests that the characteristics of the disease are defined in part by the sequence of the infecting prion.[1,2] The molecular mechanism by which prion diseases develop is thought to involve a transformation from the molecule's normal cellular conformation (PrP^{c}) to an aggregated species, the scrapie form (PrP^{Sc}), also reviewed by Caughey.[3] This aggregate, which develops into the characteristic plaque found in the brain of infected individuals, has a significantly higher proportion of β-sheet than observed in PrP^{c}, but relatively little is known about how this or the remaining helical structure is organised. Thus, in spite of intense research into the conformational behaviour of the molecule, the nature of the structural change that converts PrP^{c} to PrP^{Sc}, and the mechanism of infection remain unknown.[4] The paucity of such information seriously limits attempts to understand the disease process and thus restricts the development of a rational approach to diagnosis and therapy. Since PrP^{c} itself is a potential target

† L.F.H. & S.M.W. contributed equally to the work.

Abbreviation used: PrP, prion protein.

E-mail address of the corresponding author: pbayley@nimr.mrc.ac.uk

for pharmacological intervention, high resolution structural information is essential for design and evaluation of appropriate therapeutic agents.

There have been extensive NMR studies on the solution structure of PrP (reviewed[5]) while, by contrast, the X-ray crystallographic approach has been limited by difficulties in crystallising the protein. However, the crystal structure of a truncated mutant of human PrP has recently been reported.[6] Surprisingly, this work showed that a covalently linked dimer had been formed, apparently during the crystallisation process. We report here the crystal structure of residues 121–231 of the monomeric form of the C-terminal domain of the sheep prion protein. This domain has been intensively studied by physical and structural methods (reviewed in Refs. 5,7). It is known to support transmission of neuropathological conditions in transgenic mice[8,9] and in further truncated forms it is itself toxic, causing ataxia and cerebral degeneration.[10] Given the evidence that the structural transition of prion protein from its normal conformation to its amyloid structure is accompanied by a significant increase in β-sheet[11–14] we have examined our crystallographic model to identify segments of the sheep PrP sequence with the potential to form extended β-sheet structure. We then consider how the PrP molecule may utilise such β-structural elements in initiation of the self-association of PrP leading to the formation of PrP fibrils typical of TSE diseases.

Plasmid construction and protein purification

The sequences of sheep, human and hamster PrP are closely similar, but have different numbering. For simplicity, the hamster numbering scheme is applied throughout; thus the disulphide is Cys179 → Cys214, except for specific reference to the sheep sequence, for which italicised numbering is used.

The plasmid encoding ovPrP*(94-233)*, ARQ allele, with an N-terminal linker containing a His6 tail was described previously.[15] The naturally occurring mutation, *R151C*, was introduced using the following oligonucleotides; 5′-CGTTACTGAT ACTCCTGACAATGATAGCACTTTTG-3′ and 5′-CAAAAGTGCTATCATTGTCAGGAGTATCAGT AACGG-3′ *via* the QuikChange Site Directed Mutagenesis system (Stratagene). The integrity of the gene sequence was verified by DNA sequencing. The resulting protein, ovPrP*(94-233) R151C*, was expressed, purified, refolded and re-oxidised as described previously for doppel proteins. This refolding method results in the formation of the native internal disulphide bond, with the novel cysteine residue protected by a mixed disulphide with glutathione, as confirmed by mass spectrometry. The protein is non-glycosylated, and lacks the GPI anchor. Protein concentration was determined spectrophotometrically using the calculated molar extinction coefficient at 280 nm of 21,170 M^{-1} cm^{-1}.[16] SDS PAGE gels of the stock protein solution after storage revealed that, as with the human PrP protein,[6] the molecule His_6-PrP(90-231) had undergone proteolytic cleavage. Mass spectroscopy suggests that the truncation occurs initially at residue His111, and eventually yields Gly119 → Ala231 as the major product.

Crystallisation and data collection

Initial crystal screening experiments using the automated microbatch technique (*IMPAX 1-5* robot, Douglas Instruments) yielded tiny clusters and plates in several conditions with various salts (i.e. sodium citrate, sodium malonate, ammonium sulphate, sodium/potassium phosphate) as precipitant. Optimisation of these conditions was achieved using the hanging-drop vapour-diffusion technique. Drops (1 μl) were set up at a protein concentration of 7 mg/ml and mixed with an equal volume of reservoir solution. Thin plate-like crystals grew from sodium potassium phosphate solutions over the range 0.8–1.3 M (pH 7.4–8.6). Data were initially collected in-house on a crystal grown from 0.9 M phosphate (pH 8.6) at 10 °C and flash-frozen in liquid nitrogen after serial transfer into mother liquor augmented with 25% glycerol as cryoprotectant. High-resolution data were subsequently collected from the same crystal at SRS, Daresbury. Data were integrated and scaled using DENZO and Scalepack, respectively.

Structure determination, refinement and associated modelling

The crystals of sheep PrP(121-231) grew in a plate-like habit and diffracted to better than 2 Å Bragg spacing. A data set that was 93% complete overall (20–2.05 Å) was collected at SRS, Daresbury. The structure of these crystals was solved by molecular replacement using AMORE,[17] based on the crystal structure of the human prion protein, 1I4m[6] as a search model. In the first step of the molecular replacement calculation the C-terminal helix (residues 195–230) was omitted from the search model because of its role in "swapping over" with the corresponding helix in the human PrP dimer. This helix was subsequently positioned within the monomer by rigid-body fitting after least-squares superposition with the corresponding segment established by NMR analysis. The structure was built using O[18] and refined using a combination of REFMAC5[19] and CNS.[20] Crystallographic statistics are presented in Table 1. Subsequent modelling calculations, unrestrained by X-ray terms, were carried out using the CHARMM program[21] utilising the toph19/param19 potential.[22] Energy minimisations were carried out using combinations of steepest descent and adopted basis Newton Raphson methods.[21]

Table 1. Crystallographic statistics

Space group	$P2_12_12$
Unit cell (Å)	$a = 85.1$, $b = 29.0$, $c = 45.9$
Resolution (Å)	20–2.05
Completeness (%)	93.2 (83.7)
$R_{sym.}$ (%)	10.3 (46.5)
R_{work} (%)	27.3
R_{free} (%)	31.9
rms bonds (Å)	0.007
rms angles (°)	1.2

The values in parenthesis are for the highest resolution bin (2.12–2.05 Å). The final dataset, for which the parameters above apply, include a low-resolution pass as well as the higher resolution data collected at the SRS. The low resolution set was collected in-house on a Raxis II detector with the same crystal later used for the SRS collection. Merging of both sets of data adds ca 2% to R_{sym} but significantly enhances the completeness of the intense, low resolution terms and, perhaps unsurprisingly, produces better quality electron density maps. This factor likely accounts for the crystallographic refinement statistics being somewhat higher than would be expected given the quality of the electron density maps.

The crystal structure of sheep PrP globular domain

The sheep protein has approximate dimensions of 55 Å × 35 Å × 25 Å, and the crystals contain 45% solvent. The domain contains three helices (helix-1: 143–154; helix-2: 172–194; helix-3: 200–225), and one short segment of double-stranded anti-parallel β-sheet (129–131:163–161). The temperature factors (Figure 1) indicate that helices 1,2 and 3 are all well defined, and that a relatively compact core is formed by helix-1, the C-terminal region of helix-2 and the N-terminal region of helix-3. The latter two elements are limited by the intramolecular disulphide bond linking Cys179 to Cys214, which has an SS dihedral angle of −90°. The N-terminal segment prior to residue 123 is partially disordered and residues 124–137 have relatively high thermal factors. There is evidence from the difference electron density for alternative conformations between 132 and 137. The subsequent sequence was built continuously as far as residue 230.

Overall the electron density maps are of good quality as is illustrated by the omit density for a single $[HPO_4]^{2-}$ ion. (Preliminary results suggest this ion is only weakly bound.) This ion is located between helices 1 and 3. It forms salt bridges to Arg208 and Lys204, and makes hydrogen bonds to Glu146 (carboxylate) and to two amide main-chain nitrogen atoms at 142 and 143, as shown in Figure 2A. An additional side-chain salt bridge is seen at Asp147:Arg151; the interaction Arg164:Gln168 (sheep PrP) is present in the human prion as a salt bridge, Arg164:Glu168. The salt bridge Arg148:Glu152 present in the human PrP dimer, is absent from the sheep PrP structure, owing to the inclusion of the mutation Arg148Cys. A number of water molecules, some partially buried, have been identified, mediating hydrogen bonds that presumably help stabilise this conformation of the PrP^c molecule.

Comparison with human dimer

Figure 2B shows the conformation of the sheep prion protein C-terminal segment for comparison with that of the dimeric form of human

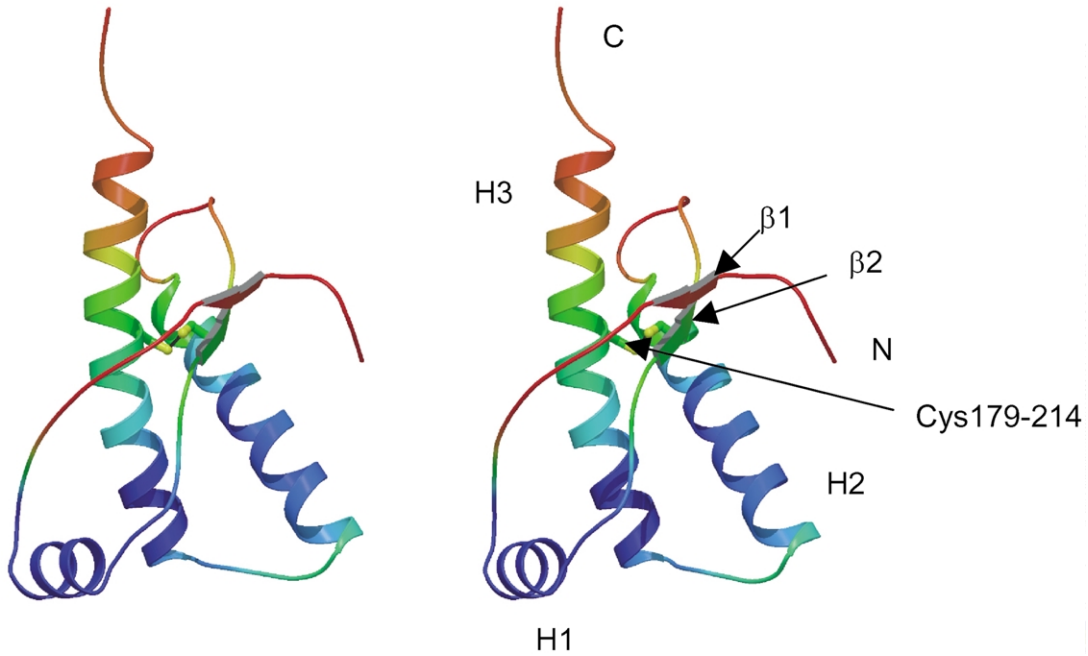

Figure 1. Stereo view of residues 123–230 of the crystal structure of the globular domain of sheep PrP showing the secondary structural elements, and intramolecular cystine bridge. The colour coding represents the experimentally determined temperature factors (Figure drawn with Bobscript).

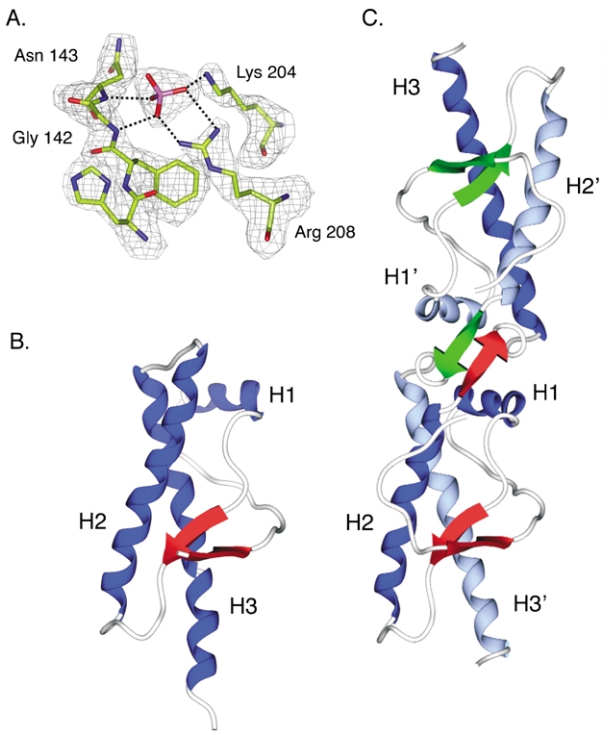

Figure 2. A, Portion of a CNS all omit map covering the vicinity of the phosphate ion linking the segment of the polypeptide at the immediate N terminus of helix-1 with the middle section of helix-3. (Liganding to Glu146 is not shown for clarity, see the text.) B, Schematic representation of the sheep PrP molecule. The helices, labelled H1–H3, are shown in blue, and the short segments of anti-parallel β-sheet are shown in red. C, Schematic representation of the helix-swapped dimer structure of the human prion protein.[6] The bottom half of the dimer is in the same orientation as the sheep PrP shown in B and similarly coloured, but with H3 in light blue. The dyad-related monomer is at the top and its β-strands are coloured in green. The helices for the dyad-related molecule are distinguished by a prime. The exchange of H3 and H3′ is accompanied by the formation of an additional segment of anti-parallel β-sheet, coloured in red and green (Figure drawn with Spock).

PrP(119-231) (Figure 2C), obtained from crystals grown under conditions containing 3 M NaCl (pH 8.3).[6] In this structure, helix-3 is swapped between two PrP molecules, so that the structure of both helices and the local interactions in the monomer are preserved. This unusual structural reorganisation requires the exchange of the 179–214 disulphide bond that links helices 2 and 3, from an intramolecular to intermolecular configuration with the same chirality as in the monomer. The dimer molecule also contains an intermolecular anti-parallel β-sheet through residues 190–194, and the corresponding segment related by crystal symmetry. In the monomeric sheep PrP structure, these residues are part of the C-terminal end of helix-2. The dimerisation in the human PrP structure and the formation of the intermolecular β-sheet is dependent on the partial unwinding of the C-terminal end of helix-2. This is therefore, a limited $\alpha \rightarrow \beta$ transition, restricted to this local region.

In the human and sheep prion crystal structures the extended loops have distinctive properties. In the human prion C-terminal domain the N-terminal segment 119–135 is relatively ordered, a consequence of its crystal contacts, while the segment 190–194 involved in the intermolecular β-sheet contacts has high thermal factors. In the sheep PrP the pattern is reversed, the segment 121–135 has high thermal factors, whereas the segment 190–195 (helix-2 in the sheep PrP) is well defined. This contrasting pattern of behaviour is not completely explained by crystal contacts. In the case of the human prion the N-terminal residues do make crystal contacts but without forming β-sheet structure. Curiously in both crystal structures the extended loops are relatively poorly ordered when they are participating in β-strands.

The $\alpha \rightarrow \beta$ conversion process of PrP itself is most frequently observed *in vitro* in the range pH 4–7[23–26] and has been postulated to be induced *in vivo* due to the low pH of endosomal compartments.[27,28] Such conditions appear unlikely to induce disulphide reduction or exchange under physiological conditions, and such reactions do not appear to be a necessary requirement for PrP^{Sc} formation.[29] However, the observations that the structure adopted by residues from 188 to 200 in the human PrP appears to be of lower relative stability compared to the rest of the structure, suggesting that a group of four threonine residues within this segment has an intrinsic propensity to undergo a local $\alpha \rightarrow \beta$ transition. This suggests the feasibility of this $\alpha \rightarrow \beta$ transition occurring under conditions that promote PrP^{Sc} formation, independent of a disulphide exchange reaction. This region could then be an additional locus for β-structure nucleation.

Comparison with NMR structures

The structures of PrP protein constructs from numerous mammalian species have been reviewed in detail.[5] There are relatively few sequence differences between the sheep/human PrP domain, and these are mainly conservative changes, i.e. 138Leu/Ile; 143Asn/Ser, 166Val/Met, 168Gln/Glu; 185Val/Ile; 204Ile/Val, but including 155His/Tyr with a more significant difference in side-chain. Figure 3 shows the recent NMR structure of the human PrP C-terminal domain,[30] compared to the crystal structure of the sheep PrP domain. Least-squares superposition of C^{α} atoms of residues 125–225 of the representative human PrP NMR structure (1hjm.pdb) and the sheep crystal structure shows an rms difference of 1.79 Å, but there is a closer similarity in secondary structure. The three helices H1–H3 together superpose with an rms difference of 1.41 Å (52 C^{α} atoms), while the pairwise superposition of helices yields rms values

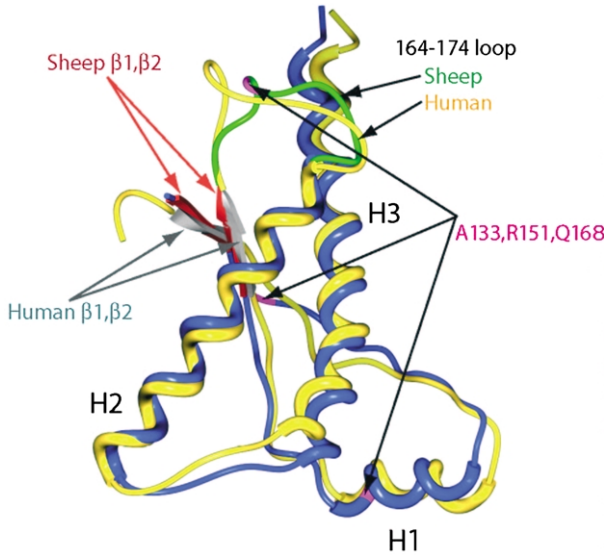

Figure 3. Comparison of the crystal structure of the globular domain of the ARQ allele of sheep PrP (blue) and the NMR structure of human PrP (yellow: 1hjm.pdb): least-squares superimposition of common residues, with an rms difference = 1.73 Å for 100 C^{α} atoms. In addition to the three helices, the intramolecular β-sheet (arrows, β1:129–131; β2:161–163) is shown in red for sheep PrP, and grey for human PrP. The YYR epitope is at 162–164. The loop 164–174 between β2 and H2, is shown in green for sheep PrP. The three polymorphic residues of sheep (A133,R151,Q168), are shown in magenta (Figure drawn with Spock).

of 0.95 Å (H1–H2, 26 atoms), 1.22 Å (H2–H3, 43 atoms), and 1.37 Å (H1–H3, 35 atoms). The main contribution to these differences is that the initial residues of helix-2 at the N terminus of sheep PrP are more regular than comparable residues in the human PrP NMR structure, and the C-terminal structure of helix-3 is somewhat more curved in the crystal structure, than is seen in this, and other NMR structures. Small differences are also evident in the helix packing. The polypeptide loops linking the helices are similar in overall position, but show significant variation in conformation. There is particular interest in the loop between the second β-strand (161–163) and the start of helix-2. This loop segment, relatively poorly defined by NMR and showing intermediate values of backbone thermal factors in the sheep (and human) crystal structures, has been postulated to be the region of additional protein–protein interactions, potentially those involving protein-X, postulated as a facilitator of the $PrP^{c} \rightarrow PrP^{Sc}$ conversion.[31–33] There are other considerable variations between the NMR and X-ray structure determinations for residues at either N or C termini, and also at the side-chain level for the S–S bridge. Further comparisons are limited by the absence of water molecules in the NMR determined structures; a number of side-chain conformations are likely to be affected by solvent packing and H-bond contacts.

Potential β-strand polymerisation sites

There are two specific observations from the available crystallographic structures of PrP^{c} that may be relevant to the development of β-sheet containing oligomeric species during the formation of the aggregated PrP^{Sc} form. First, from the sheep PrP crystal structure we find that the segment 129–131 forms an anti-parallel β-sheet with a symmetry-related molecule (see Figure 4A). By means of this crystallographic symmetry interaction, the two-stranded anti-parallel β-sheet in each molecule (129–131 and 161–163) becomes a four-stranded anti-parallel sheet extending across two molecules. The dimer contact region is relatively flexible and largely polar, with the most significant contact being that between the two symmetry-related Met129 residues. This observation suggests that the 129–131 segment of the sheep PrP could represent a potential locus (L1) for further β-structure development, and hence help to nucleate β-mediated intermolecular interactions *in vivo*.[34] Intriguingly, there is an exclusive correlation between the occurrence of the human disease, new variant CJD, and the homozygous expression of the Met129 isoform of PrP.[35]

Secondly, as described above, the dimeric structure of human PrP shows monomers interacting through a β-sheet created by a local change in conformation.[6] The highly conserved amino acid sequence, residues 188–201 (TVTTTTKGENFTET) has several interesting features that appear relevant to this region undergoing a change in conformation under suitable perturbing conditions. It contains seven threonine residues; the four consecutive threonine residues contribute to the β-sheet segment in the human PrP^{c} structure. In the sheep PrP^{c} structure, these residues, plus Thr188, all make hydrogen bonds with the main-chain carbonyl groups of helix-2, potentially strengthening what may otherwise be a relatively unstable structure. The hydroxyl of Thr199 hydrogen bonds to the peptide NH of 201–202 in helix-3, while that of Thr201 is directed away from the helix into solution. In contrast with sheep PrP, in the human PrP structure helix-2 terminates at residue 190, with Thr191, Thr192 and Thr193 located on the β-strand, with their side-chains directed into solvent. The hydrogen bonding of Thr199 hydroxyl is to the swapped helix-3. The potential of these threonine residues to make different networks of hydrogen bonds, as seen in the sheep and human PrP structures, may facilitate the shift in this local $\alpha \rightarrow \beta$ conformation. The fact that the seven threonine residues are invariant across a wide variety of species[36] suggests a functional role, possibly in facilitating localised conformational plasticity in this part of the PrP molecule. This leads us to propose that, under suitable perturbing conditions, residues 188–200 of the monomeric sheep PrP molecule may be restructured so that residues 190–194 adopt a β-strand conformation, while retaining the

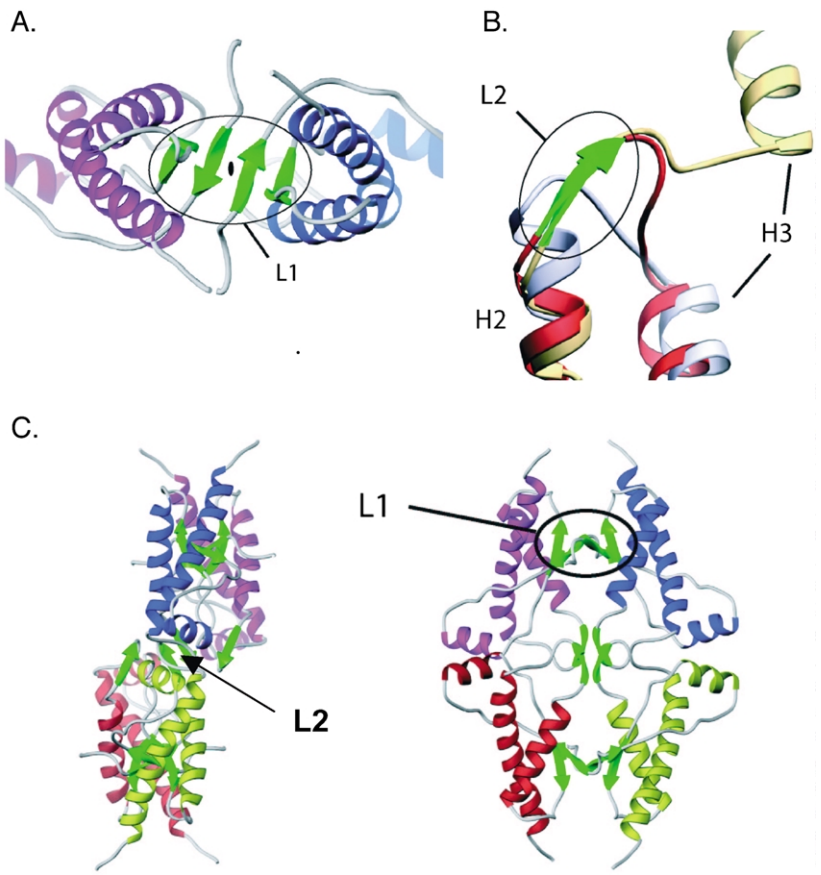

Figure 4. A, Schematic representation of the crystallographic dyad-mediated lattice contact between two monomers in the sheep PrP crystals. The four-stranded anti-parallel β-sheet is coloured in green and labelled locus L1. B, Schematic representation showing the superposition of three structures in the region linking helices 2 and 3: the helix-swapped human PrP dimer (yellow), the sheep PrP crystal structure (white, this paper), and the remodelled sheep PrP (red), see the text. The segment of β-strand, present in the human PrP structure, and modelled into sheep PrP, is coloured in green, and marked as the L2 locus. C, Two orthogonal views of a tetramer of sheep PrP molecules generated through the two β-mediated loci. The mauve and blue coloured monomers (with β-sheet coloured green), as well as the red and yellow pair, are generated by the crystallographic dyad in the sheep PrP crystal structure and the interface is marked as the L1 locus. The blue and yellow pairs are generated by remodelling and symmetry generation based on that observed in the human PrP crystal structure. This second association is mediated through the L2 locus (Figure drawn with Ribbons).

similarity in position of helix-3 between the sheep PrP structure and that seen in the helix-swapped model of the human PrP.

We have tested this possibility, using molecular modelling of the PrP monomer structure. The Thr190–Thr199 segment was reoriented such that residues Thr190–Thr193 followed the trace of the corresponding residues in the human PrP dimer structure, generating a second β-strand locus (L2) (Figure 4B). The remaining segment (Lys-194 to Thr-199) was allowed to relax to a local minimum using constrained energy minimisations, applied to a dimer of the restructured sheep monomer, generated using transformations derived from the human structure. The procedure establishes that the local α → β change can indeed be incorporated in the monomeric structure without perturbing helix-3. A dimer of the restructured sheep monomer was generated from the human PrP dimer model, showing that a non-covalent dimer of a modified sheep PrP structure can in principle be generated through a β-strand interface, using residues 190–193.

The new dimer of "modified monomers" of sheep PrP (see molecules coloured blue and yellow in Figure 4C) is a flat structure with approximate dimensions of 80 Å × 60 Å × 25 Å. It has two exposed β-strands, centred on Met129 and labelled L1, that were described earlier as mediating lattice contacts in the sheep PrP crystal structure. Application of the crystal dyad transformation observed in the sheep PrP to the modified dimer structure at L1 generates a tetramer as shown in Figure 4C, which could in principle undergo further oligomerisation.

Discussion

The structure of the sheep prion protein is the first monomeric PrP structure to be obtained by X-ray crystallography. It is of particular interest in view of the fact that scrapie, the disease of sheep, predates the more recent identification of TSEs by more than 200 years.[37] The absence of evidence of an infection of humans from sheep was taken to indicate a species-specific barrier that prevented transmission of the disease *via* the human food chain. Our results show that the structure of the globular domain of sheep PrP correlates quite closely with structures of many other species, including the human PrP^{c}. Thus there is no detectable structural property of the cellular form of sheep PrP that might account for its lack of transmissibility to humans.

It is widely recognised that numerous proteins,

and polypeptide sequences derived from them, can polymerise through repeated β-strand interactions to form an amyloid structure.[38] In the case of prion diseases, the aggregated material PrP^{Sc}, containing PrP with an enhanced proportion of β-structure,[11–14] undergoes partial proteolytic processing to PrP(27-30), prior to amyloid fibril formation.[39] In addition, the prion diseases are unique amongst the amyloidoses in being transmissible serially between animals, although the process remains obscure. Thus, although amyloid fibrils evidently exhibit structural features in common, there may be different mechanisms of formation and the fibril structure may not be identical in all cases.

The identity of distinctive residues in the globular domain affected by the $PrP^{c} \rightarrow PrP^{Sc}$ conversion has been indicated by changes in the immunological properties of the protein. Epitopes in the N-terminal region of PrP^{c} (residues 90–120) become buried in the PrP^{Sc} form:[40] conversely, a YYR epitope, probably at 162–164, that is inaccessible in PrP^{c} becomes accessible in PrP^{Sc}.[41] Other evidence of the importance of this region comes from analysis of the protease-resistant PrP^{Sc} material of the related Gerstmann–Straüssler–Scheinker syndrome as containing peptides of sequence ~88–153.[42] Also a distinctive β-helix ultra-structure of the region 141–176 is suggested by imaging of a two-dimensional crystal form derived from PrP27-30.[43] These data indicate the likely, but not necessarily exclusive, involvement of residues in the N-terminal and central portion of the sequence of PrP(90-231) as contributing to the β-rich region of PrP^{Sc}.

The crystal structure of the sheep PrP molecule reveals two potential loci of β-structure propagation within the monomer. At least two such loci are necessary for the formation of an open polymeric assembly. First, the structure reveals an important lattice contact involving the β-strand 129–131 (L1). The associated crystallographic dyad generates a four-stranded, intermolecular β-sheet. In view of the small number of intermolecular contacts at this site, this interface appears likely to confer only a weak propensity for dimerisation of PrP in solution. However, we speculate that this may be an initial contact from which a more extensive interface develops under conditions favouring β-structure formation.

Secondly, comparison of our X-ray structure of sheep PrP with that of the human suggests that a limited $\alpha \rightarrow \beta$ conformational change may occur in the C terminus of helix-2. Applying the dimer dyad axis seen in the human PrP structure to the restructured sheep monomer generates a non-covalent β-mediated dimer (L2). Although there are clearly other loci where *de novo* β-structure generation could occur, L1 and L2 are two identified sites where β-structure could be propagated from pre-existing β-strands within the predominantly α-structured monomer.

It may be noted that dimerisation of PrP essentially in the α-form has been reported, following treatment of PrP(90-231) with low concentrations of detergent at neutral pH, and this non-covalent association has been postulated to precede the $\alpha \rightarrow \beta$ conversion reaction.[44] Either of the two β regions discussed here could promote the formation of such a dimer as an intermediate species in the subsequent overall more extensive $\alpha \rightarrow \beta$ transformation. Quantitatively, this transformation requires a change in conformation of approximately 18 α-helical residues in the globular domain, plus any additional residues involved in *de novo* β-structure formation.[11–13] This estimate is considerably larger than the minimal estimates of β-structure in the loci L1 and L2. Nonetheless, this analysis reinforces the potential role of these two loci as initiators of molecular associations that are subsequently driven by a more substantial $\alpha \rightarrow \beta$ conformational change. This process corresponds to the model of nucleated conformational conversion, as proposed for the involvement of structurally fluid intermediates acting as nuclei in prion amyloid formation.[45–48]

In addition, any structural model of fibril formation from PrP must have the spatial ability to accommodate the N terminus of the PrP(90-231) molecule, and the post- translational glycosyl modifications, that occur (at Asn181 and Asn197) in the physiologically relevant forms of PrP. Glycosylation has been shown to slow down fibrillar conversion in a model peptide system,[49] consistent with some involvement of the L2 region in the conversion process.

Overall the crystal structure of sheep PrP provides the basis for detailed comparison with other PrP structures, and facilitates the design of structurally directed experiments to further define the biochemical and biophysical mechanisms of PrP conformational conversion and prion disease. The analysis of the crystal structure of the sheep PrP, and the associated modelling studies in comparison with the dimeric structure of human PrP illustrate the small extent of conformational adjustment within the monomeric PrP^{c} structure required to produce a potentially oligomeric nucleating unit, and this may be important for the PrP amyloid forming process.

Atomic coordinates

The coordinates have been deposited with the Protein Data Bank under the ID Code 1UW3.pdb.

Acknowledgements

We thank Alan Bennett, IAH for providing the sheep construct pARQ#9PrP, Stephen Martin for advice on characterising PrP preparations, and Steve Gamblin and Steve Smerdon for helpful

discussions and preparation of Figures. We are grateful to Daresbury SRS for access to synchrotron time.

References

1. Prusiner, S. B. (1998). Prions. *Proc. Natl Acad. Sci. USA*, **95**, 13363–13383.
2. Jackson, G. S. & Collinge, J. (2001). The molecular pathology of CJD: old and new variants. *Mol. Pathol.* **54**, 393–399.
3. Caughey, B. (2001). Prion protein interconversions. *Philos. Trans. R. Soc. Lond. B Biol. Sci.* **356**, 197–200. discussion 200–202.
4. Chesebro, B. (1999). Prion protein and the transmissible spongiform encephalopathy diseases. *Neuron*, **24**, 503–506.
5. Wuthrich, K. & Riek, R. (2001). Three-dimensional structures of prion proteins. *Advan. Protein Chem.* **57**, 55–82.
6. Knaus, K. J., Morillas, M., Swietnicki, W., Malone, M., Surewicz, W. K. & Yee, V. C. (2001). Crystal structure of the human prion protein reveals a mechanism for oligomerization. *Nature Struct. Biol.* **8**, 770–774.
7. Glockshuber, R. (2001). Folding dynamics and energetics of recombinant prion proteins. *Advan. Protein Chem.* **57**, 83–105.
8. Fischer, M., Rulicke, T., Raeber, A., Sailer, A., Moser, M., Oesch, B. *et al.* (1996). Prion protein (PrP) with amino-proximal deletions restoring susceptibility of PrP knockout mice to scrapie. *EMBO J.* **15**, 1255–1264.
9. Flechsig, E., Shmerling, D., Hegyi, I., Raeber, A. J., Fischer, M., Cozzio, A. *et al.* (2000). Prion protein devoid of the octapeptide repeat region restores susceptibility to scrapie in PrP knockout mice. *Neuron*, **27**, 399–408.
10. Shmerling, D., Hegyi, I., Fischer, M., Blattler, T., Brandner, S., Gotz, J. *et al.* (1998). Expression of amino-terminally truncated PrP in the mouse leading to ataxia and specific cerebellar lesions. *Cell*, **93**, 203–214.
11. Caughey, B. W., Dong, A., Bhat, K. S., Ernst, D., Hayes, S. F. & Caughey, W. S. (1991). Secondary structure analysis of the scrapie-associated protein PrP27-30 in water by infrared spectroscopy. *Biochemistry*, **30**, 7672–7680.
12. Safar, J., Roller, P. P., Gajdusek, D. C. & Gibbs, C. J., Jr (1993). Thermal stability and conformational transitions of scrapie amyloid (prion) protein correlate with infectivity. *Protein Sci.* **2**, 2206–2216.
13. Pan, K. M., Baldwin, M., Nguyen, J., Gasset, M., Serban, A., Groth, D. *et al.* (1993). Conversion of alpha-helices into beta-sheets features in the formation of the scrapie prion proteins. *Proc. Natl Acad. Sci. USA*, **90**, 10962–10966.
14. Baldwin, M. A., Pan, K. M., Nguyen, J., Huang, Z., Groth, D., Serban, A. *et al.* (1994). Spectroscopic characterization of conformational differences between PrPC and PrPSc: an alpha-helix to beta-sheet transition. *Philos. Trans. R. Soc. Lond. B Biol. Sci.* **343**, 435–441.
15. Whyte, S. M., Sylvester, I. D., Martin, S. R., Gill, A. C., Wopfner, F., Schatzl, H. M. *et al.* (2003). Stability and conformational properties of doppel, a prion-like protein, and its single-disulphide mutant. *Biochem. J.* **373**, 485–494.
16. Gill, S. C. & von Hippel, P. H. (1989). Calculation of protein extinction coefficients from amino acid sequence data. *Anal. Biochem.* **182**, 319–326.
17. Navaza, J. (1994). AMoRe: an automated package for molecular replacement. *Acta Crystallog. sect. A*, **50**, 157–163.
18. Jones, T. A., Zhou, J. Y., Cowan, S. W. & Kjeldgaard, M. (1991). Improved methods for building protein models in electron density maps and the location of errors in these models. *Acta Crystallog. sect. A*, **47**, 110–119.
19. Collaborative Computational Project, Number 4 (1994). CCP4 suite: programs for protein crystallography. *Acta Crystallog. sect. D*, **50**, 760–763.
20. Brunger, A. T., Adams, P. D., Clore, G. M., DeLano, W. L., Gros, P., Grosse-Kunstleve, R. W. *et al.* (1998). Crystallography and NMR system: a new software suite for macromolecular structure determination. *Acta Crystallog. sect. D Biol. Crystallog.* **54**, 905–921.
21. Brooks, B., Bruccoleri, R. E., Olafson, B. D., States, D. J., Swaminathan, S. & Karplus, M. (1983). CHARMM—a program for macromolecular energy minimization and dynamics. *J. Comput. Chem.* **4**, 187–217.
22. Neria, E., Fischer, S. & Karplus, M. (1996). Simulation of activation free energies in molecular systems. *J. Chem. Phys.* **105**, 1902–1921.
23. Swietnicki, W., Petersen, R., Gambetti, P. & Surewicz, W. K. (1997). pH-dependent stability and conformation of the recombinant human prion protein PrP(90-231). *J. Biol. Chem.* **272**, 27517–27520.
24. Hornemann, S. & Glockshuber, R. (1998). A scrapie-like unfolding intermediate of the prion protein domain PrP(121-231) induced by acidic pH. *Proc. Natl Acad. Sci. USA*, **95**, 6010–6014.
25. Swietnicki, W., Morillas, M., Chen, S. G., Gambetti, P. & Surewicz, W. K. (2000). Aggregation and fibrillization of the recombinant human prion protein huPrP90-231. *Biochemistry*, **39**, 424–431.
26. Zou, W. Q. & Cashman, N. R. (2002). Acidic pH and detergents enhance *in vitro* conversion of human brain PrPC to a PrPSc-like form. *J. Biol. Chem.* **277**, 43942–43947.
27. Caughey, B., Raymond, G. J., Ernst, D. & Race, R. E. (1991). N-terminal truncation of the scrapie-associated form of PrP by lysosomal protease(s): implications regarding the site of conversion of PrP to the protease-resistant state. *J. Virol.* **65**, 6597–6603.
28. Borchelt, D. R., Taraboulos, A. & Prusiner, S. B. (1992). Evidence for synthesis of scrapie prion proteins in the endocytic pathway. *J. Biol. Chem.* **267**, 16188–16199.
29. Welker, E., Raymond, L. D., Scheraga, H. A. & Caughey, B. (2002). Intramolecular *versus* intermolecular disulfide bonds in prion proteins. *J. Biol. Chem.* **277**, 33477–33481.
30. Calzolai, L. & Zahn, R. (2003). Influence of pH on NMR structure and stability of the human prion protein globular domain. *J. Biol. Chem.* **278**, 35592–35596.
31. Telling, G. C., Scott, M., Mastrianni, J., Gabizon, R., Torchia, M., Cohen, F. E. *et al.* (1995). Prion propagation in mice expressing human and chimeric PrP transgenes implicates the interaction of cellular PrP with another protein. *Cell*, **83**, 79–90.
32. Ryou, C., Prusiner, S. B. & Legname, G. (2003). Cooperative binding of dominant-negative prion protein to kringle domains. *J. Mol. Biol.* **329**, 323–333.
33. Kaneko, K., Zulianello, L., Scott, M., Cooper, C. M., Wallace, A. C., James, T. L. *et al.* (1997). Evidence for protein X binding to a discontinuous epitope on the

cellular prion protein during scrapie prion propagation. *Proc. Natl Acad. Sci. USA*, **94**, 10069–10074.
34. Riek, R., Hornemann, S., Wider, G., Billeter, M., Glockshuber, R. & Wuthrich, K. (1996). NMR structure of the mouse prion protein domain PrP(121-231). *Nature*, **382**, 180–182.
35. Will, R. G., Ironside, J. W., Zeidler, M., Cousens, S. N., Estibeiro, K., Alperovitch, A. *et al.* (1996). A new variant of Creutzfeldt–Jakob disease in the UK. *Lancet*, **347**, 921–925.
36. Wopfner, F., Weidenhofer, G., Schneider, R., von Brunn, A., Gilch, S., Schwarz, T. F. *et al.* (1999). Analysis of 27 mammalian and 9 avian PrPs reveals high conservation of flexible regions of the prion protein. *J. Mol. Biol.* **289**, 1163–1178.
37. Brown, P. & Bradley, R. (1998). 1755 and all that: a historical primer of transmissible spongiform encephalopathy. *Bmj*, **317**, 1688–1692.
38. Dobson, C. M. (2001). Protein folding and its links with human disease. *Biochem. Soc. Symp.*, 1–26.
39. Nguyen, J. T., Inouye, H., Baldwin, M. A., Fletterick, R. J., Cohen, F. E., Prusiner, S. B. & Kirschner, D. A. (1995). X-ray diffraction of scrapie prion rods and PrP peptides. *J. Mol. Biol.* **252**, 412–422.
40. Peretz, D., Williamson, R. A., Matsunaga, Y., Serban, H., Pinilla, C., Bastidas, R. B. *et al.* (1997). A conformational transition at the N terminus of the prion protein features in formation of the scrapie isoform. *J. Mol. Biol.* **273**, 614–622.
41. Paramithiotis, E., Pinard, M., Lawton, T., LaBoissiere, S., Leathers, V. L., Zou, W. Q. *et al.* (2003). A prion protein epitope selective for the pathologically misfolded conformation. *Nature Med.* **9**, 893–899.
42. Tagliavini, F., Lievens, P. M., Tranchant, C., Warter, J. M., Mohr, M., Giaccone, G. *et al.* (2001). A 7-kDa prion protein (PrP) fragment, an integral component of the PrP region required for infectivity, is the major amyloid protein in Gerstmann–Straussler–Scheinker disease A117V. *J. Biol. Chem.* **276**, 6009–6015.
43. Wille, H., Michelitsch, M. D., Guenebaut, V., Supattapone, S., Serban, A., Cohen, F. E. *et al.* (2002). Structural studies of the scrapie prion protein by electron crystallography. *Proc. Natl Acad. Sci. USA*, **99**, 3563–3568.
44. Jansen, K., Schafer, O., Birkmann, E., Post, K., Serban, H., Prusiner, S. B. & Riesner, D. (2001). Structural intermediates in the putative pathway from the cellular prion protein to the pathogenic form. *Biol. Chem.* **382**, 683–691.
45. Come, J. H., Fraser, P. E. & Lansbury, P. T., Jr (1993). A kinetic model for amyloid formation in the prion diseases: importance of seeding. *Proc. Natl Acad. Sci. USA*, **90**, 5959–5963.
46. Eigen, M. (1996). Prionics or the kinetic basis of prion diseases. *Biophys. Chem.* **63**, A1–18.
47. Serio, T. R., Cashikar, A. G., Kowal, A. S., Sawicki, G. J., Moslehi, J. J., Serpell, L. *et al.* (2000). Nucleated conformational conversion and the replication of conformational information by a prion determinant. *Science*, **289**, 1317–1321.
48. Kelly, J. W. (2000). Mechanisms of amyloidogenesis. *Nature Struct. Biol.* **7**, 824–826.
49. Bosques, C. J. & Imperiali, B. (2003). The interplay of glycosylation and disulfide formation influences fibrillization in a prion protein fragment. *Proc. Natl Acad. Sci. USA*, **100**, 7593–7598.

Edited by K. Nagai

(Received 28 July 2003; received in revised form 10 November 2003; accepted 19 December 2003)